

DEMONSTRATION OF ARTIFICIAL SPIN STATES USING SUB-HARMONIC INJECTION LOCKING IN AlN-on-Si LENGTH-EXTENSIONAL MODE MEMS SELF-SUSTAINING OSCILLATOR

Tahmid Kaisar^{1*}, S M Enamul Hoque Yousuf¹, Nicolas Casilli²,

Mina Rais-Zadeh^{3,4}, Soumyajit Mandal⁵, Cristian Cassella², and Philip X.-L. Feng^{1*}

¹Electrical & Computer Engineering, University of Florida, Gainesville, FL 32611, USA

²Electrical & Computer Engineering, Northeastern University, Boston, MA 02115, USA

³Electrical & Computer Engineering, University of Michigan, Ann Arbor, MI 48109, USA

⁴Jet Propulsion Laboratory, California Institute of Technology, Pasadena, CA 91109, USA

⁵Instrumentation Division, Brookhaven National Laboratory, Upton, NY 11973, USA

ABSTRACT

We report on phase state control via injection locking phenomena in piezoelectric microelectromechanical systems (MEMS) based self-sustaining oscillators. By applying a sub-harmonic injection locking (SHIL) signal on piezoelectric AlN-on-Si (AlN/Si) length-extensional (LE) mode MEMS feedback oscillator, we create bistable phase states, which is the first demonstration of spin-mimicking up and down states of an Ising model using MEMS-based self-sustaining oscillators. In this work, we first characterize the oscillator performance, *e.g.*, phase noise and frequency stability (Allan deviation) to examine the computational capabilities of these MEMS oscillators for Ising machines. Then we explore the probabilities of getting bistable phase states with varying injection locking voltage. This bistability in phase space can be utilized to build large-scale Ising machines using coupling between MEMS oscillators. Furthermore, it enables the utilization of the MEMS oscillators as binary logic latches, where the logic value can be encoded within the phase of oscillation. Finally, we have numerically solved a 4-node Max-Cut problem with various binary weight configurations using the complex Ginzburg-Landau (CGL) model for coupled self-sustaining MEMS oscillators.

KEYWORDS

Microelectromechanical systems (MEMS), sub-harmonic injection locking (SHIL), length-extensional (LE) mode, phase noise, Allan deviation, Ising machine, Max-Cut, Ginzburg-Landau model, piezoelectric.

INTRODUCTION

As Moore's law scaling is reaching its limit, the limitations of traditional von Neumann computers in addressing crucial challenges in a modern society have sparked a quest for alternative computing and device technologies. One promising alternative is the Ising machine [1], recognized for its efficacy in solving combinatorial optimization problems (COPs) [2]. COPs are pervasive in real-world applications such as artificial intelligence, vehicle routing, and computer networking; and they often prove very challenging for traditional von Neumann computing architectures. Ising machines are engineered physical systems with the primary purpose of identifying the ground states of the Ising model (Fig. 1g-h) [3]. They have been realized through the utilization of diverse physical platforms, including superconducting

qubits [4], optical parametric oscillators [5], electrical oscillators [6-8], digital CMOS devices [8], memristors [9], and photonic simulators [10], *etc.* Unlike quantum and optical approaches, electronic oscillator Ising machines (OIMs) can function at chip scale and at room temperature, which makes it appealing for the development of low-power scalable computing hardware. OIMs often utilize SHIL to create bistable phase states that can emulate artificial Ising spins in the electrical domain, where phases of 0° and 180° (with respect to a reference signal) represent spin-up and spin-down states ($\sigma = \pm 1$), respectively.

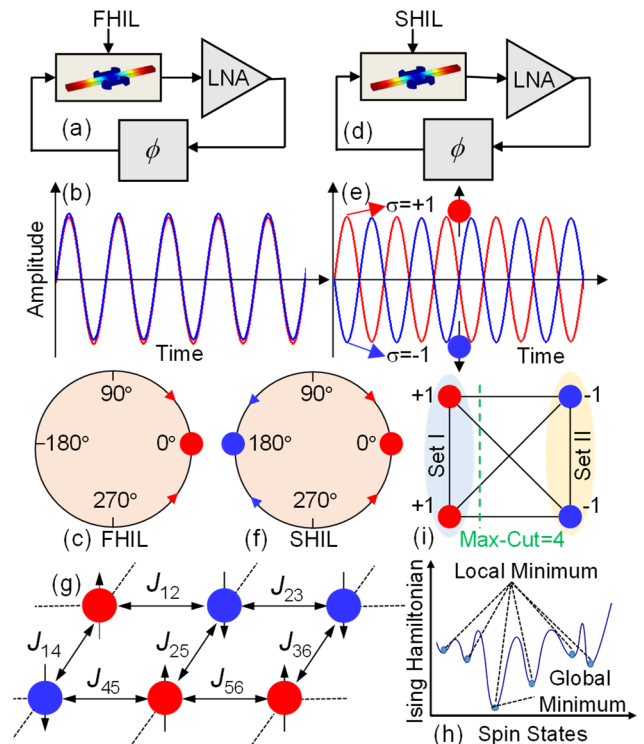


Figure 1: Illustrations of injection locking in AlN/Si MEMS self-sustaining oscillators for building Ising machines. (a)-(c) Illustration of first harmonic injection locking (FHIL) creating only one stable phase state. (d)-(f) Illustration of SHIL creating bistable phase states. (g) 2D network of an Ising model where the Ising Hamiltonian is defined as $H = -\sum J_{ik} \sigma_i \sigma_k$, with J_{ik} being the interaction between spins and σ the spin state. (h) Energy landscape. (i) A 4-node Max-Cut problem solution using the Ising model. Max-Cut is defined as a graph cut that divides the nodes of a graph into two sets (Set I and Set II in the figure) so that the number of common edges between them is maximized.

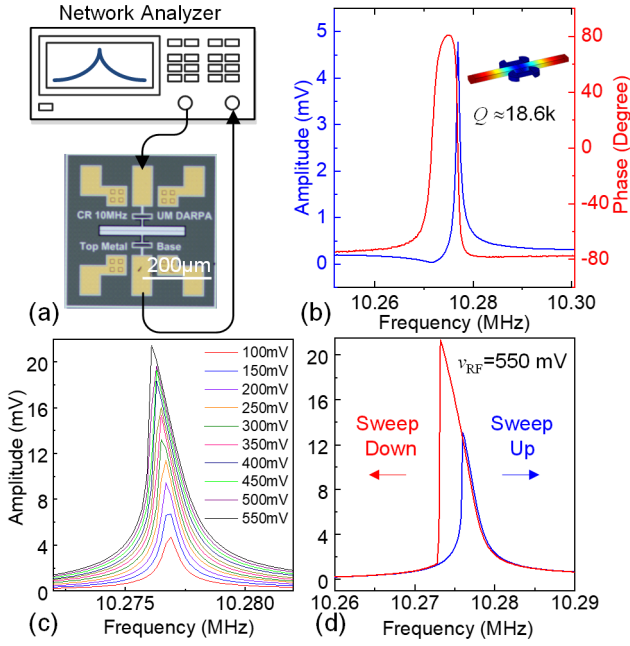


Figure 2: (a) Measurement scheme for characterizing piezoelectric transduction of AlN/Si MEMS resonator. Electrically measured (b) linear resonance at $v_{RF} = 100$ mV and (c) nonlinear resonance after electrical background subtraction at varying $v_{RF} = 100$ mV to 550 mV. (d) Measured nonlinear bifurcation with both upward (blue) and downward (red) frequency sweeps at $v_{RF} = 550$ mV.

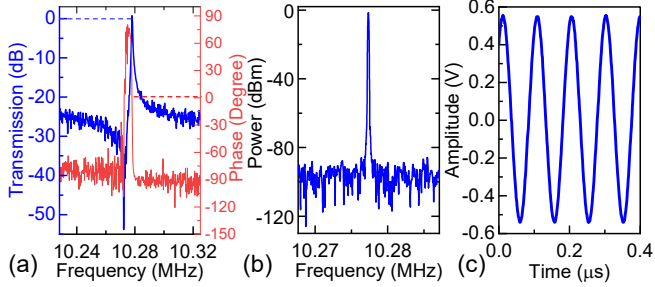


Figure 3. Measured open-loop and closed-loop responses. (a) Calibration of Barkhausen criteria in open-loop response. (b) Closed-loop spectrum. (c) Stable oscillations.

Although significant endeavors of analytical and experimental studies have been done to predict injection locking behavior in LC and ring oscillators [7-8,11], no experimental work has been done on SHIL in MEMS based self-sustaining oscillators towards creating artificial spins. Towards the goal of building MEMS OIMs, in this work, we first explore the SHIL in AlN/Si piezoelectric LE mode MEMS self-sustaining oscillators [12] to create artificial spin states (Fig. 1d-f). When our MEMS oscillator is perturbed by only first harmonic injection locking (FHIL) signal at ω_0 , the output shows a constant phase locking configuration for multiple runs (Fig. 1a-c). After we apply $\omega_{inj} = 2\omega_0$ for an injection locking voltage $v_{inj} > 60$ mV, the phase distribution shows equiprobable and bistable phase portraits while measuring over multiple runs as predicted from Adler's equation [13]. To demonstrate capabilities of solving COPs, we numerically solve 4-node Max-Cut (well-known NP-hard problem) problems (Fig. 1i) having various binary weight configurations utilizing nonlinear

dynamics of coupled AlN/Si MEMS feedback oscillators.

DEVICE CHARACTERIZATION

We first characterize the fundamental LE mode resonance (at 10.28 MHz) of AlN/Si MEMS resonator by performing two-port network analysis (Fig. 2a). The device shows a quality factor of $Q \approx 18,600$ in its linear regime at an RF drive of $v_{RF} = 100$ mV (Fig. 2b). As v_{RF} increases from 100 mV to 550 mV, the device exhibits Duffing softening nonlinearity (Fig. 2c) and clear bifurcation (Fig. 2d).

We then build a self-sustaining AlN/Si MEMS oscillator by calibrating/tuning open-loop measurement [12] to satisfy the Barkhausen criteria (Fig. 3a). Next, we close the loop and measure stable oscillation in both frequency and time domains (Fig. 3b-c). We examine the oscillator performance by measuring its phase noise and frequency stability (Allan deviation). Investigating phase noise is crucial in determining computational capabilities of OIMs as noise in the system can alter the probability of the OIM to determine the optimal solution of COPs. Below 180 Hz offset frequency, the phase noise decreases with $1/f^3$ power law that is dominated by flicker ($1/f$) noise. Measured phase noise at 1 kHz offset is -115 dBc/Hz (Fig. 4a). Next, we calculate the Allan deviation (Fig. 4c) of the oscillator from measured frequency fluctuations for 4.5 hours (Fig. 4b). The Allan deviation data show short-term frequency stability of $\sigma_A \approx 5 \times 10^{-9}$ at averaging time $\tau_A = 1$ s, and long-term stability of $\sigma_A \approx 4 \times 10^{-7}$ at $\tau_A = 1000$ s.

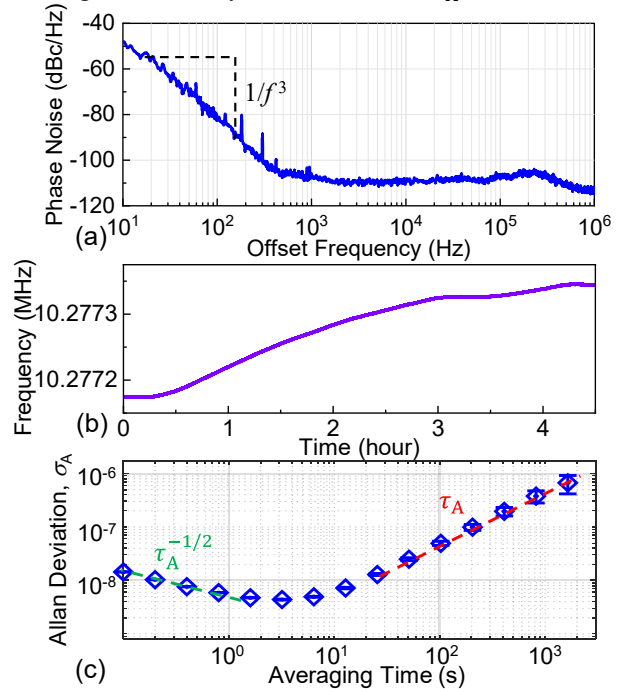


Figure 4. Oscillator performance characterization. (a) Phase noise of 10 MHz MEMS oscillator. (b) Measured frequency variation over 4.5 hours. (c) Allan deviation computed from the frequency tracking data in (b). It follows a $\tau_A^{-1/2}$ power law at short averaging time (0.1s-2s) and a τ_A power law at long averaging time (30s-1000s).

RESULTS AND ANALYSIS

The binary degrees of freedom (DoF) in the phase space of OIMs result from SHIL. We apply a $2\omega_0$ injection

locking signal (SHIL) to the oscillator (Fig. 5) and observe the output on an oscilloscope. The SHIL is applied from a function generator as an external input and added to the self-oscillating signal (at ω) using a power combiner (splitter). While $v_{inj}=0\text{mV}$, the oscillator is free running. Then we increase v_{inj} from 25mV to 95mV with 10mV step. The phase of the oscillator referenced to a sinusoidal signal with the same frequency exhibits bistable phase states with both in-phase (0°) and out-of-phase (180°) injection-locking configurations for two different runs at $v_{inj}=65\text{mV}$ (Fig. 6a). This bistability in phase space can provide an ideal method to emulate Ising spin where in-phase and out-of-phase configurations represent spin-up and spin-down states, respectively. Because of the frequency mismatch between the oscillator output and injection locking signal, there is a threshold value of the injection voltage below which no stable solution can be found. We observe that after $v_{inj}=60\text{mV}$, the bistability in phase state starts to appear and phase distribution becomes narrower. The amplitude heterogeneity in a SHIL oscillator distorts the Lyapunov function that samples the Hamiltonian of the problem to solve, in some circumstances causing failures in proper convergence [14]. Eventually, the phase fluctuates between two stable states because of the stochasticity (phase noise) in the system. Below this threshold voltage, the phase of the oscillator shows a wider distribution in phase space for multiple runs (Fig. 6b).

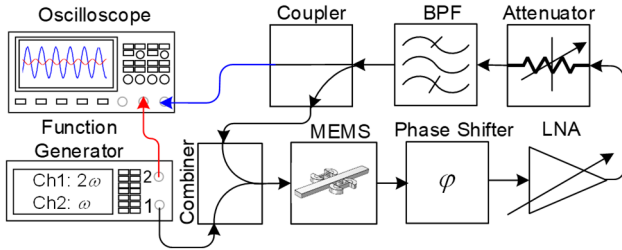


Figure 5: Block diagram of the measurement system for SHIL. Oscillator phase is measured with respect to a reference signal (Chanel 2) from the function generator.

The equation of motion of a nonlinear self-sustaining MEMS oscillator under an external injection locking signal can be written in non-dimensional form as

$$\ddot{x}_i + \frac{1}{Q}\dot{x}_i + x_i + \eta_i x_i \dot{x}_i^2 + k_i x_i^3 = H_i(t) + F(x_i, \dot{x}_i). \quad (1)$$

Here, x_i is the displacement of the MEMS resonator, $H_i(t)$ is an external injection locking signal, F is the internal feedback of the self-sustaining oscillator, η_i is the nonlinear damping coefficient, and k_i is the Duffing nonlinear coefficient. The left-hand side of the equation represents a set of uncoupled van der Pol Duffing resonator with a Q factor, and nonlinear damping where $k_i x_i^3$ is the reactive nonlinear term that represents stiffening or softening of the spring constant causing an amplitude dependent shift (detuning) of the resonant frequency.

We use secular perturbation theory to analyze Eq. (1). First, we assume non-dimensional time, $t = \omega_0 \tilde{t}$, where \tilde{t} is the real time and ω_0 is the resonant frequency. We define the small parameter $\epsilon \equiv \frac{1}{Q} \ll 1$, and then we perform a perturbation expansion and allow the amplitude and phase of oscillations to vary on the slow time scale, $T = \epsilon t$. We can describe this variation by the slow time complex amplitude,

$A(T) = a(T)e^{i\theta(T)}$, where a and θ are the amplitude and phase of oscillation, respectively. After we set the secular terms to be zero at the second order of the expansion, we obtain a first order complex differential equation which describes the slow time dynamics as

$$\frac{dA_i}{dT} = \frac{1}{2} \frac{A_i}{|A_i|} - \frac{1}{2} A_i + j(\delta_i + k_i |A_i|^2) A_i - h_{ni} A_i^*{}^{(n-1)}, \quad (2)$$

where δ_i is the linear frequency detuning, h_{ni} is the injection locking term, $j = \sqrt{-1}$, A_i^* is the complex conjugate of A_i , and $n=2$ for SHIL. The oscillator dynamics in Eq. (2) is a modified variant from the CGL model, which is also used for studying synchronization in coupled-oscillator systems [15]. Equation (2) describes the envelope (amplitude and phase) of individual uncoupled oscillators. It can be separated into real and imaginary sub-equations that yield both the amplitude and phase dynamics of individual oscillators.

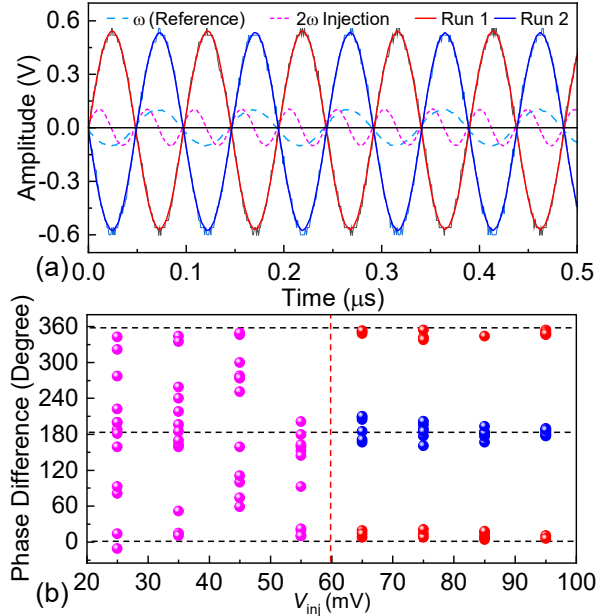


Figure 6: Sub-harmonic injection locking (SHIL) scenario. (a) Bistable phase states to mimic artificial spins with $v_{inj}=65\text{mV}$ for two different runs. (b) Distribution of phase with increasing v_{inj} for 12 different runs. The oscillator is forced to bistable states (blue & red) for $v_{inj}>60\text{mV}$.

Under the assumption of weak coupling among the oscillators, we add the coupling term $j \sum_{k=1}^N \beta_{ik} (A_i - A_k)$ in Eq. (2) for the coupled oscillator network, where β_{ik} is the coupling coefficient. For this weakly coupled nonlinear system, the complex equations for amplitude and phase dynamics of the CGL model can be reduced to phase dynamics of the oscillators. To demonstrate that our coupled nonlinear AlN/Si MEMS oscillators can solve the Ising model, we utilize this system to solve Max-Cut problems numerically. Figure 7 displays several 4-node Max-Cut problems at various binary weight configurations. Using our CGL model, we have confirmed the accuracy of each solution by comparing it with solutions generated by other OIMs [7] and the solution obtained by a Max-Cut approximate solution algorithm [16]. Each node of the Max-Cut problem is represented by a single AlN/Si MEMS oscillator. The solid lines between the oscillator nodes represent a weight of 1, while missing a line of connection represents a weight of 0. When node 1 is connected to the

three other nodes, the system energy is minimized while node 1 is out of phase with the others (Fig. 7a-b). Figure 7i shows an all-to-all connected scheme where we can have 6 degenerate solutions in which any two oscillators are out of phase with the other two oscillators. Figure 7j demonstrates one of the six possible solutions.

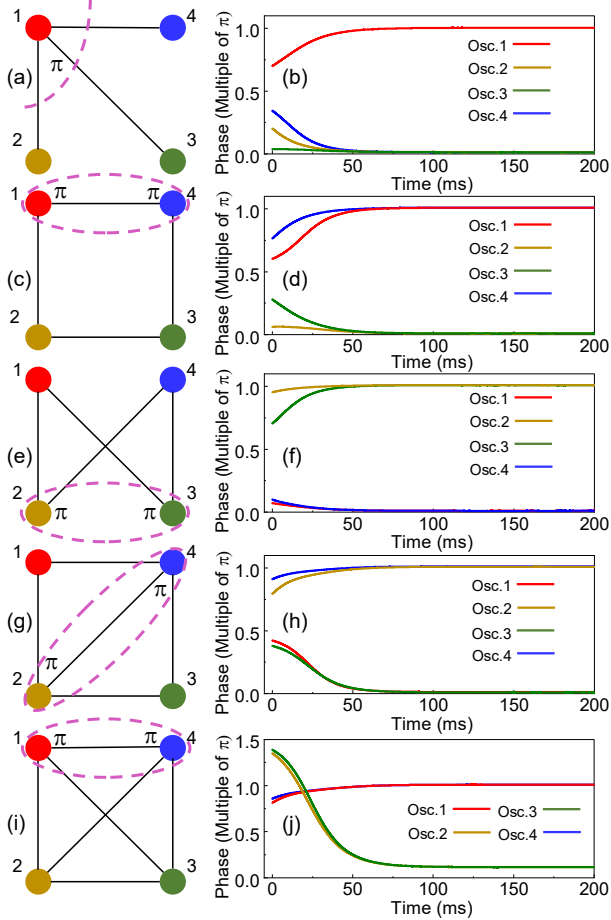


Figure 7. Numerically solving 4-node Max-Cut problems with different binary weight configurations using the CGL model. The corresponding phase dynamics for each configuration are shown in the plot on its right. Phases are synchronized to 0 or π due to the application of SHIL.

CONCLUSIONS

In summary, we have reported artificial spin states using SHIL in piezoelectric AlN/Si LE mode MEMS self-sustaining oscillators. We have explored the probabilities of attaining bistable phase states with varying SHIL for multiple runs. We have found that bistability in phase states of our MEMS oscillator cannot be obtained below $v_{inj} = 60\text{mV}$. Finally, we have numerically solved Max-Cut problems with binary weight configurations to demonstrate the capability of coupled nonlinear MEMS oscillators to solve optimization problems. These nonlinear MEMS resonators can be integrated with a programmable CMOS ASIC [17] to build large-scale CMOS-MEMS analog Ising computer for solving NP-hard problems which are not easily solvable by mainstream von Neumann computers.

ACKNOWLEDGEMENTS

We are thankful to the National Science Foundation (NSF) for the financial support through the CISE CCF-FET program (Grants #2103091 and #2103351).

REFERENCES

- [1] T. Wang, *et al.*, “Solving combinatorial optimization problems using oscillator based Ising machines,” *Natural Computing* **20**, 287-306, 2021.
- [2] A. Lucas, “Ising formulations of many NP problems,” *Frontiers in Physics* **2**, 5, 2014.
- [3] E. Ising, “Beitrag zur theorie des ferromagnetismus,” *Zeitschrift für Physik* **31**, 253-258, 1925.
- [4] F. Arute, *et al.*, “Quantum supremacy using a programmable superconducting processor,” *Nature* **574**, 505-510, 2019.
- [5] T. Inagaki, *et al.*, “A coherent Ising machine for 2000-node optimization problems,” *Science* **354**, 603-606, 2016.
- [6] N. Casilli, *et al.*, “Nonvolatile state configuration of nano-Watt parametric Ising spins through ferroelectric hafnium zirconium oxide MEMS varactors,” in *Proc. 35th IEEE MEMS*, Munich, Germany, 511-514, 2023.
- [7] J. Chou, *et al.*, “Analog coupled oscillator based weighted Ising machine,” *Scientific Reports* **9**, 14786, 2019.
- [8] H. Lo, *et al.*, “An Ising solver chip based on coupled ring oscillators with a 48-node all-to-all connected array architecture,” *Nature Electronics* **6**, 771-778, 2023.
- [9] F. Cai, *et al.*, “Power-efficient combinatorial optimization using intrinsic noise in memristor Hopfield neural networks,” *Nature Electronics* **3**, 409-418, 2020.
- [10] D. Pierangeli, *et al.*, “Large-scale photonic Ising machine by spatial light modulation,” *Physical Review Letters* **122**, 213902, 2019.
- [11] A. Neogy, *et al.*, “Analysis and design of subharmonically injection locked oscillators,” in *Proc. IEEE DATE*, Dresden, Germany, 1209-1214, 2012.
- [12] T. Kaisar, *et al.*, “Five low-noise stable oscillators referenced to the same multimode AlN/Si MEMS resonator,” *IEEE Transactions on Ultrasonics, Ferroelectrics, and Frequency Control* **70**, 1213-1228, 2023.
- [13] P. Bhansali, *et al.*, “Gen-Adler: The generalized Adler’s equation for injection locking analysis in oscillators,” in *Proc. IEEE ASP-DAC*, Yokohama, Japan, 522-527, 2009.
- [14] T. Leleu, *et al.*, “Destabilization of local minima in analog spin systems by correction of amplitude heterogeneity,” *Physical Review Letters* **122**, 040607, 2019.
- [15] A. Pikovsky, *et al.*, *Synchronization: A Universal Concept in Nonlinear Sciences*, Cambridge Nonlinear Science Series: Cambridge University Press, 2001.
- [16] M. X. Goemans, *et al.*, “Improved approximation algorithms for maximum cut and satisfiability problems using semidefinite programming,” *Journal of the ACM* **42**, 1115-1145, 1995.
- [17] T. Kaisar, *et al.*, “Digitally programmable CMOS feedback ASIC for network of coupled electromechanical oscillators,” in *Proc. 2023 IEEE ISCAS*, Monterey, CA, USA, 1-5, 2023.

CONTACT

- *Tahmid Kaisar: kaisart@ufl.edu
 *Philip Feng: philip.feng@ufl.edu